DECIGO/BBO as a Probe to Constrain
Alternative Theories of Gravity

Kent Yagi[1] and Takahiro Tanaka[2]

[1] *Department of Physics, Kyoto University, Kyoto 606-8502, Japan*
[2] *Yukawa Institute for Theoretical Physics, Kyoto University,
Kyoto 606-8502, Japan*

We calculate how strongly one can constrain the alternative theories of gravity with deci-Hz gravitational wave interferometers such as DECIGO and BBO. Here we discuss Brans-Dicke theory and massive graviton theories as typical examples. We consider the inspiral of compact binaries composed of a neutron star (NS) and an intermediate mass black hole (IMBH) for Brans-Dicke (BD) theory and those composed of a super massive black hole (SMBH) and a black hole (SMBH) for massive graviton theories. Using the restricted 2PN waveforms including spin effects and taking the spin precession into account, we perform the Monte Carlo simulations of 10^4 binaries to estimate the determination accuracy of binary parameters including the Brans-Dicke parameter ω_{BD} and the graviton Compton length λ_g. Assuming a $(1.4, 10)M_\odot$ NS/BH binary of SNR $= \sqrt{200}$, the constraint on ω_{BD} is obtained as $\omega_{BD} > 2.32 \times 10^6$, which is 300 times stronger than the estimated constraint from LISA observation. Furthermore, we find that, due to the expected large merger rate of NS/BH binaries of $O(10^4)$ yr^{-1}, a statistical analysis yields $\omega_{BD} > 3.77 \times 10^8$, which is 4 orders of magnitude stronger than the current strongest bound obtained from the solar system experiment. For massive graviton theories, assuming a $(10^6, 10^5)M_\odot$ BH/BH binary at 3 Gpc, one can put a constraint $\lambda_g > 3.35 \times 10^{20}$ cm, on average. This is three orders of magnitude stronger than the one obtained from the solar system experiment. From these results, it is also understood that DECIGO/BBO is a very powerful tool for constraining alternative theories of gravity.

Many challenges have been made to modify gravitational theory from general relativity in order to explain the current acceleration of the universe.[1] In this paper, we focus on two simple possibilities, Brans-Dicke theory[2] and massive graviton theories.[3]–[6] Brans-Dicke theory is a scalar-tensor theory[7] of the simplest type. This theory is parameterised by the so-called Brans-Dicke parameter ω_{BD} and approaches general relativity in the limit $\omega_{BD} \to \infty$. The current strongest bound on this parameter, $\omega_{BD} > 4 \times 10^4$, is obtained by the solar system experiment using the Saturn probe satellite Cassini.[8] It measured the Shapiro time delay, which corresponds to measuring the spatial metric deviation from general relativity. Another constraint on ω_{BD} has been obtained from orbital period decay rate of a binary PSR J1141-6545, which consists of a neutron star and a white dwarf.[9] Since there exists scalar dipole radiation in Brans-Dicke theory, the orbital evolution changes from the one in general relativity, whose information is implemented in the orbital period decay rate. Bhat et al.[9] found that constraint becomes $\alpha_0^2 \equiv \frac{1}{2\omega_{BD}+3} < 2.1 \times 10^{-5}$ for Brans-Dicke theory, which corresponds to $\omega_{BD} > 2.38 \times 10^4$. Although this bound is 2 times weaker than the Cassini one, it has distinct meaning since it gives a direct

constraint on scalar dipole radiation.

On the other hand, massive graviton theories by definition introduce a finite mass m_g to the graviton. Verification of Kepler's third law in the solar system experiment puts the lower bound on the graviton Compton length, $\lambda_g \equiv h/m_g c$, as $\lambda_g > 2.8 \times 10^{17}$ cm.[10]

Estimate for the constraint on alternative theories of gravity using gravitational waves from inspiral compact binaries has been studied in several papers.[11]–[14] Recently, Berti et al.[15] calculated the constraint on ω_{BD} and λ_g with LISA,[16],[17] using restricted 2PN waveforms and performed Monte Carlo simulations. Following their analysis, we improved their calculation by including the spin-spin coupling σ, small orbital eccentricity, and spin precession effects.[18] Under the assumption of the so-called *simple precession*[19],[20] and when we restrict our calculation for circular binary orbits, we obtained the constraints on ω_{BD} and λ_g as $\omega_{BD} > 6944$ using a $(1.4, 1000) M_\odot$ NS/BH binary of SNR $= \sqrt{200}$ and $\lambda_g > 4.86 \times 10^{21}$ cm using a $(10^7, 10^6) M_\odot$ BH/BH binary at 3 Gpc. When we include eccentricities, we found that the constraint on ω_{BD} is unaffected as long as we include prior information whilst the one on λ_g becomes $\lambda_g > 3.10 \times 10^{21}$ cm. Therefore we can say that the effects of eccentricities are not so strong for both cases. At the same time, Stavridis and Will[21] estimated the constraint on λ_g for a circular BH/BH binary including both spins of binary objects and taking spin precession into account. For a BH/BH binary of $(10^6, 10^6) M_\odot$ at 3 Gpc, they obtained $\lambda_g > 5 \times 10^{21}$ cm when the spin-spin precession effect is taken into account and $\lambda_g > 4 \times 10^{21}$ cm when it is not taken into account. To compare our results with their ones, we estimated the constraint on λ_g with a $(10^6, 1.1 \times 10^6) M_\odot$ circular BH/BH binary under simple precession, in which the spin-spin precession effect is neglected, and obtained the constraint $\lambda_g > 3.7 \times 10^{21}$ cm.[18] Although we cannot directly compare these two results, it seems that our results are consistent with the ones obtained by Stavridis and Will.[21] There is also a recent work done by Yunes and Pretorius[22] in which they proposed a new framework, *the parametrised post-Einsteinian framework*, to perform gravitational wave tests of alternative theories of gravity.

Following our previous paper,[18] we estimate the possible constraint on ω_{BD} and λ_g obtained by detecting gravitational waves from the inspiral of precessing compact binaries using deci-Hz space-borne gravitational wave interferometers such as DECIGO[23]–[25] and BBO.[26],[27] These detectors are most sensitive in the frequency band between 0.1 Hz and 1 Hz, and the noise levels are about four orders of magnitude lower than that of LISA. These detectors have a huge number of compact binaries as promising sources. (Because of that, high precision cosmology using them is also expected.[28]) In this paper we perform the analysis assuming DECIGO noise curve but almost the same results will also apply to BBO. Here, we restrict our attention to circular binaries since the lower bounds on ω_{BD} and λ_g are not much affected by the inclusion of eccentricity into binary parameters. (The upper bound on ω_{BD}, if detected, can be affected by including eccentricity, though.) Since the detection rate of NS/BH mergers is expected to be $O(10^4)$ for DECIGO/BBO, we add a statistical analysis, which improves the constraint on the deviation from general relativity. Our results are only approximate estimates in that we do not take

the errors coming from the use of approximate waveforms into account[29] and also due to the limitation of the validity of the Fisher analysis.[30]

First we review the basic plan of DECIGO (DECi-hertz Interferometer Gravitational wave Observatory) and show the noise curve. DECIGO is a planned space gravitational wave antenna mission.[23],[25] It consists of four constellations of three drag free satellites which keep the triangular shape throughout the flight. These three satellites form Fabry-Perot interferometers with separation 1000 km. DECIGO can detect gravitational waves from both astrophysical and cosmological sources mainly between 0.1–10 Hz. Among them, compact binaries are the promising sources, although the primary goal of the mission is to detect primordial gravitational wave background at the level of $\Omega_{\rm GW} = 10^{-16}$. For LISA frequency band, such small signals are completely obscured by the foregrounds generated by white-dwarf binaries. Since this foreground noise has cutoff frequency around 0.2 Hz,[31] DECIGO has a much better chance to detect the primordial gravitational wave background.

The instrumental noise spectral density for DECIGO is given by[32]

$$S_h^{\rm inst}(f) = 5.3 \times 10^{-48} \left[(1 + x^2) + \frac{2.3 \times 10^{-7}}{x^4 (1 + x^2)} + \frac{2.6 \times 10^{-8}}{x^4} \right] {\rm Hz}^{-1},$$

where $x = f/f_p$ with $f_p \equiv 7.36$ Hz. The three terms on the right-hand side represent the shot noise, the radiation pressure noise and the acceleration noise, respectively.

Besides instrumental noise, there are three main foreground confusion noises: galactic white dwarf binaries $S_h^{\rm gal}(f)$,[33] extra-galactic white dwarf binaries $S_h^{\rm ex-gal}(f)$,[31] and neutron star binaries $S_h^{\rm NS}(f)$.[34] The noise spectral densities for the first two confusion noises are given in Ref. 18). Following Ref. 34), the noise spectral density for NS binaries is estimated as $S_h^{\rm NS}(f) = 1.3 \times 10^{-48} (f/1{\rm Hz})^{-7/3}$, where we have set the cosmological parameters to $\Omega_m = 0.3$, $\Omega_\Lambda = 0.7$ and $H_0 = 72$ km/s/Mpc.

Then, the total noise spectral density for DECIGO becomes

$$S_h(f) = \min \left[\frac{S_h^{\rm inst}(f)}{\exp(-k N_f / T)}, S_h^{\rm inst}(f) + S_h^{\rm gal}(f) \mathcal{R}(f) \right] + S_h^{\rm ex-gal}(f) \mathcal{R}(f) + 0.01 \times S_h^{\rm NS}(f),$$

(1)

where the factor $\mathcal{R}(f) \equiv \exp\{-2 (f/0.05\ {\rm Hz})^2\}$ represents the cutoff of the WD/WD binary confusion noise. We put the factor 0.01 in front of $S_h^{\rm NS}(f)$, which represents the fraction of gravitational waves that cannot be removed after foreground subtraction. Namely, we assume that 99% of the gravitational waves from neutron star binaries can be identified and removed. N_f is the number density of galactic white dwarf binaries per unit frequency given in Ref. 18). $k \simeq 4.5$ is the average number of frequency bins that are lost when each galactic binary is fitted out and T represents the observation time which we fix as 1 yr. The noise curve (1) is shown in Fig. 1 as a thick solid curve. We introduce low and high cutoff frequencies at $f_{\rm low} = 10^{-3}$ Hz and $f_{\rm high} = 100$ Hz, respectively. Although it has not been estimated rigorously, it might be possible to extend the noise curve on lower frequency side down to 10^{-4}–10^{-5} Hz.[32] This bound comes from the limitation of controlling the mirror
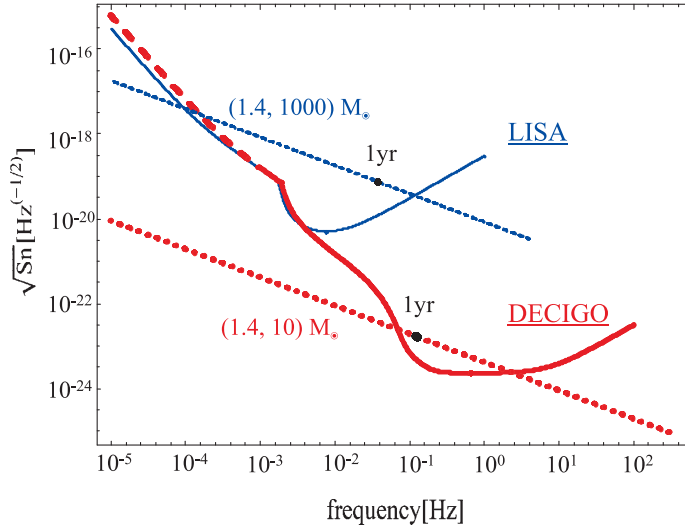
Fig. 1. Noise spectral density for DECIGO (thick solid curve) and LISA (thin solid curve). It might be possible to extend the DECIGO noise curve down to 10^{-5} Hz[32] (thick dashed curve). We also show the amplitudes of gravitational waves from a $(1.4, 1000)M_\odot$ (thin dotted line) and a $(1.4, 10)M_\odot$ (thick dotted line) NS/BH binary with each SNR set to $\rho = 10$ for 1 yr observation before coalescence. Each dot labeled "1 yr" represents the frequency at 1 yr before coalescence.

positions. This extension is shown as a thick dashed curve in Fig. 1. We also show the noise curve of LISA as a thin solid curve for comparison. Thin dotted line and thick dotted line each, respectively, represent the amplitude of gravitational waves from a $(1.4, 1000)M_\odot$ and a $(1.4, 10)M_\odot$ NS/BH binary of SNR $\rho = 10$ with 1 yr observation before coalescence. Each dot labeled "1 yr" represents the frequency at 1 yr before coalescence.

We used the matched filtering analysis to estimate the determination accuracy of the binary parameters. There are 14 parameters in total: the chirp mass $\ln \mathcal{M}$, the dimensionless mass ratio η; the coalescence time t_c, the coalescence phase ϕ_c; the distance to the source D; the spin-orbit and spin-spin coupling coefficients, β and σ; the directional cosine between the orbital and spin angular momenta κ, the precession angle parameter α_c; the direction of the source (θ_S, ϕ_S); the initial direction of the total angular momentum (θ_J, ϕ_J); finally, ω_{BD}^{-1} or λ_g^{-1}, depending on which theory we are aiming to constrain. We calculate the inverse of the Fisher matrix numerically, assuming stationary and Gaussian noise. Integration is performed from f_{in} to f_{fin}, where $f_{in} = \max\{f_{low}, f_{1yr}\}$ and $f_{fin} = \min\{f_{high}, f_{ISCO}\}$, respectively. f_{1yr} is the frequency at 1yr before coalescence and f_{ISCO} is the one at the innermost stable circular orbit (ISCO). First we performed the pattern-averaged estimate of the errors in determination of the parameters for binaries with various masses, in which we have averaged over the directions of the source and the orbital angular momentum, and the spins of the binary constituents are assumed to be zero. We set SNR $= 10$ for Brans-Dicke theory and $D_L = 3$ Gpc for massive graviton theory. We also performed the

Table I. Results of error estimation with DECIGO in Brans-Dicke theory for various mass NS/BH binaries. We performed pattern-averaged estimates, using only one detector and fixing the SNR to 10.

masses	f_{in} (Hz)	f_{fin} (Hz)	ω_{BD} (10^6)	$\Delta \ln \mathcal{M}$ (10^{-5})	$\Delta \ln \eta$ (%)	$\Delta \beta$	$\Delta \sigma$
$(1.4, 10)M_\odot$	0.118	100	1.342	0.978	2.78	0.190	2.18
$(1.4, 50)M_\odot$	0.0776	85.6	0.2662	2.34	2.64	0.106	1.09
$(1.4, 100)M_\odot$	0.0651	43.36	0.1899	2.34	1.87	0.0485	0.563
$(1.4, 400)M_\odot$	0.0460	10.95	0.04244	4.96	1.85	0.0133	0.250

Table II. Comparison of the constraints on ω_{BD} and other physical quantities for a $(1.4, 10)M_\odot$ binary with DECIGO and a $(1.4, 1000)M_\odot$ binary with LISA. We performed pattern-averaged analyses and SNRs are fixed to 10 for both cases.

masses and detector	ω_{BD} (10^6)	$\omega_{\text{BD}}^{\text{uncor}}$ (10^6)	N_{GW} (10^6)	$v_{1\text{yr}}$	f_{in} (Hz)	f_{fin} (Hz)
$(1.4, 10)M_\odot$, DECIGO	1.34	332	5.9	0.027	0.118	100
$(1.4, 1000)M_\odot$, LISA	0.00821	21.6	1.8	0.083	0.0366	1.00

Monte Carlo simulations for 10^4 binaries, distributing $(\theta_{\text{S}}, \phi_{\text{S}}, \theta_{\text{J}}, \phi_{\text{J}}, \kappa, \alpha_c)$ randomly, both with and without the precession effect. We set the fiducial values to $t_c = \phi_c = \omega_{\text{BD}}^{-1} = \lambda_g^{-1} = 0$ with $(m_{\text{NS}}, m_{\text{BH}}) = (1.4, 10)M_\odot$ of SNR = 10 (for pattern-averaged estimate) or SNR = $\sqrt{200}$ (for Monte Carlo simulations) for Brans-Dicke theory, and $(m_{\text{BH}}, m_{\text{BH}}) = (10^6, 10^5)M_\odot$ at $D_L = 3$ Gpc for massive graviton theories. For the analysis without the spin precession effect, the fiducial values of β and σ are set to 0. When we take it into account, we set the dimensionless spin parameter $\chi \equiv S/m^2$ to 0 and 0.5 for the lighter and heavier bodies of binaries, respectively, where S is the magnitude of the spin angular momentum. We include prior information on β and σ when calculating Fisher matrices. See Ref. 18) for more details.

In Table I, we show the pattern-averaged results of binary parameter estimation errors for Brans-Dicke theory with $(1.4, 10)M_\odot$, $(1.4, 50)M_\odot$, $(1.4, 100)M_\odot$ and $(1.4, 400)M_\odot$ NS/BH binaries of SNR = 10. (It seems that SNRs of $O(10)$ are too small in performing the Fisher analysis.[30] However, constraints for higher SNR binaries are obtained by just scaling in proportional to SNR.) It can be seen that smaller mass binaries give stronger constraints on ω_{BD}. This can be understood as follows. The velocities of binaries at 1 yr before coalescences are slower for smaller mass binaries. Since Brans-Dicke theory gives dipole correction to binary gravitational waves, this correction is -1PN order. Therefore, when we fix SNRs, this contribution is larger for slower binaries, which makes the constraints stronger. Comparing these results with the ones in Ref. 18), we can say that DECIGO has better ability in constraining ω_{BD} compared to LISA. To be more explcit, let us compare the constraint from $(1.4, 10)M_\odot$ with DECIGO and the one from $(1.4, 1000)M_\odot$ with LISA. This mass parameter is an optimised choice for each detector to constrain Brans-Dicke theory. First, we compare the uncorrelated constraint $\omega_{\text{BD}}^{\text{uncor}}$ which is calculated directly from the Fisher matrix (not the inverse of it) and represents the possible constraint when the degeneracies between ω_{BD} and other parameters have

Table III. Results of error estimation in massive graviton theory for BH/BH binaries at 3 Gpc with various masses. We performed pattern-averaged estimates using only one detector.

masses	$f_{\rm in}$ (mHz)	$f_{\rm fin}$ (mHz)	SNR	λ_g (10^{20} cm)	$\Delta \ln \mathcal{M}$ (%)	$\Delta \ln \eta$	$\Delta \beta$	$\Delta \sigma$
$(10^6, 10^6) M_\odot$	1.0	2.20	1338	1.014	14.0	2.46	9.40	2.50
$(10^6, 10^5) M_\odot$	1.0	4.00	2044	1.270	1.19	1.69	9.10	2.44
$(10^5, 10^5) M_\odot$	1.0	22.0	4909	1.133	0.0286	0.930	7.00	1.69
$(10^5, 10^4) M_\odot$	1.0	40.0	3021	0.4066	4.51×10^{-3}	0.823	6.20	1.88
$(10^4, 10^4) M_\odot$	1.0	220.0	29569	0.3852	3.54×10^{-4}	0.924	6.96	1.68

been solved completely.[15] Table II shows that the former constraint is stronger than the latter by more than 1 order of magnitude. There are 2 reasons for this, (1) the number of gravitational wave cycles $N_{\rm GW}$ are greater and (2) the velocity at 1 yr before coalescence $v_{\rm 1yr}$ is slower. From Table II, we can see that $N_{\rm GW}$ for the former case is about 3 times greater compared to the latter case. On the other hand, $v_{\rm 1yr}$ for the former one is 3 times slower than the latter. Since the -1PN correction term in the phase is proportional to v^{-2}, this contribution is about 10 times larger for the former case. These 2 contributions make the former constraint greater by more than 1 order of magnitude. Next, we compare the constraint on $\omega_{\rm BD}$ which is calculated from the inverse of the Fisher matrices. From the table, we understand that the correlation between other parameters for the former case is weaker by more than 1 order of magnitude. We think that this comes from the difference in the width of effective frequency range of observation. From the table, we see that this frequency range is larger for the former case by more than 1 order of magnitude, which solves the degenaracies between parameters.

In Table III, we show the pattern-averaged results for massive graviton theory with $(10^6, 10^6) M_\odot$, $(10^6, 10^5) M_\odot$, $(10^5, 10^5) M_\odot$, $(10^5, 10^4) M_\odot$ and $(10^4, 10^4) M_\odot$ BH/BH binaries. In this case, larger mass binaries give stronger constraints on λ_g. This is explained from the correction to the phase velocity $v_{\rm ph}$ which is given as[18]

$$v_{\rm ph}^2 = \left(1 - \frac{1}{f^2 \lambda_g^2} \right)^{-1}. \tag{2}$$

Since more massive binaries generate lower frequency gravitational waves, these binaries give larger corrections and make the constraints stronger. However, if we increase the mass parameter too much, the SNR starts to decrease since the dynamical frequency range starts to get narrower, which makes the constraints weaker. This is why the constraint on λ_g from a $(10^6, 10^6) M_\odot$ binary is weaker compared to the one from a $(10^6, 10^5) M_\odot$ binary. In Ref. 18), we estimated the constraint from a $(10^7, 10^6) M_\odot$ binary with LISA to be 4.06×10^{20} cm. In this case LISA gives stronger constraint on λ_g than DECIGO. This is because LISA is able to detect lower frequency gravitational waves than DECIGO where the correction on $v_{\rm ph}$ is greater. If we use the extended version of DECIGO shown as thick dashed curve in Fig. 1, we found that $(10^7, 10^6) M_\odot$ binary gives a constraint of 4.05×10^{20} cm which coincides with the one obtained with LISA. This result is obvious since the frequency range of this binary is $f = 2.36 \times 10^{-5} - 4.00 \times 10^{-4}$ Hz in our case and the noise curves

Table IV. Results of error estimation in Brans-Dicke theory for $(1.4, 10)M_\odot$ NS/BH binaries. The first line shows the results of pattern-averaged estimate. We used only one detector and the SNR is fixed to 10. The second and the third lines show the results of Monte Carlo simulations. We used two detectors for the analyses and we set $\text{SNR} = \sqrt{200}$ (corresponding to $\text{SNR} = 10$ for each detector). We distribute 10^4 binaries, calculate the determination error of each parameter for each binary and take the average. The second line shows the ones without taking spin precession into account, whilst the third line represents the ones including precession. σ is included in the binary parameters for all the cases.

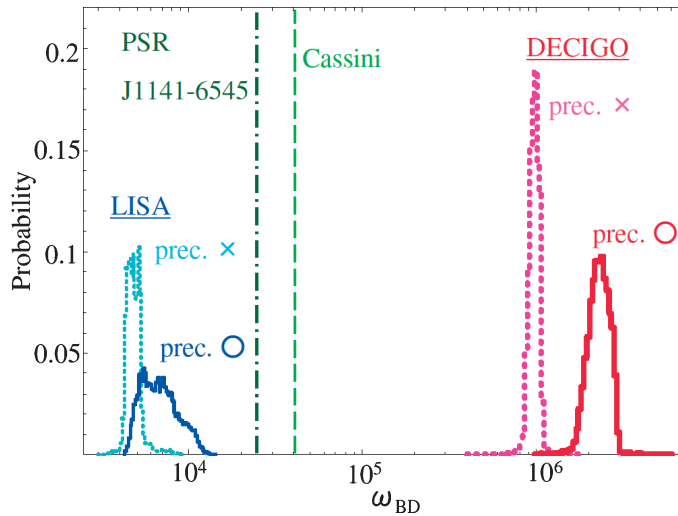| cases	ω_{BD} (10^6)	$\Delta \ln \mathcal{M}$ (10^{-5})	$\Delta \ln \eta$ (%)	$\Delta \beta$	$\Delta \ln D_L$	$\Delta \Omega_S$ (10^{-5}str)	$\Delta \sigma$
pattern-averaged	1.342	0.978	2.78	0.190	0.100	-	2.18
no precession	0.9774	1.22	3.06	0.186	1.24	3.27	2.15
including precession	2.317	0.350	0.295	0.0551	0.183	2.52	0.627

Fig. 2. Histograms showing the probability distribution of the lower bound of ω_{BD} obtained from our Monte Carlo simulations of 10^4 NS/BH binaries in Brans-Dicke theory. We take the masses of the binaries as $(1.4, 10)M_\odot$ with $\text{SNR} = \sqrt{200}$. The thick dotted one represents the estimate without precession and the thick solid one shows the one including precession using DECIGO. For comparison, we also show the results obtained in 18) for $(1.4, 1000)M_\odot$ NS/BH binaries with $\text{SNR} = \sqrt{200}$ using LISA. The thin dotted one shows the one without precession and the thin solid one represents the one including precession. The dashed line at $\omega_{\text{BD}} = 2.38 \times 10^4$ represents the constraint from PSR J1141-6545.[9]

of extended DECIGO and LISA are almost identical within this frequency range.

In Table IV, we show the results of error estimation in Brans-Dicke theory for $(1.4, 10)M_\odot$ NS/BH binaries with both pattern-averaged analysis and Monte Carlo simulations. The first row shows the ones with pattern-averaged estimate where we used only one detector and fixed the SNR to 10. The second and the third rows represent the results of Monte Carlo simulations with SNR fixed to $\sqrt{200}$. The second row shows the ones without taking spin precession into account whilst the third row shows the ones including precession. We see that inclusion of precession improves

the constraint on ω_{BD} by a factor of two. In general, binary parameters including ω_{BD} are correlated with spin parameters β and σ. When we include precession, we obtain additional information about spin which solves degeneracies and reduces the estimation errors, making the constraint stronger. Figure 2 represents the histograms showing the number fraction of binaries which give the constraint on the Brans-Dicke parameter within each bin of ω_{BD}. The thick dotted one represents the estimate without precession and the thick solid one shows the one including precession using DECIGO. For comparison, we also show the results obtained in 18) for $(1.4, 1000)M_\odot$ NS/BH binaries with SNR $= \sqrt{200}$ using LISA. The thin dotted one shows the one without precession and the thin solid one represents the one including precession. The dashed line at $\omega_{BD} = 1.47 \times 10^5$ represents the constraint from PSR J1141-6545.[9] We can see that DECIGO can put 300 times stronger constraint than LISA. The reasons are the same as the pattern-averaged analysis.

Unlike the case of LISA, these binaries are thought to be the definite sources for DECIGO. The event rate of NS/NS binary mergers is estimated to be 10^5 yr^{-1},[34] and the rate of NS/BH mergers will be about one order of magnitude smaller than that of NS/NS mergers (see Shibata et al.[35] and references therein). Therefore it is possible to put even stronger constraint by performing a statistical analysis. Defining the variance of parameter $\bar{\omega} = \omega_{BD}^{-1}$ from i-th binary as σ_i, the total variance σ is given by

$$\sigma^{-2} = \Delta T \int_0^\infty 4\pi [a_0 r(z)]^2 \dot{n}(z) \frac{d\tau}{dz} \sigma(z)^{-2} dz, \tag{3}$$

where $\Delta T = 1$ yr represents the observation time, a_0 represents the current scale factor, $r(z)$ is the comoving distance to the source, $\dot{n}(z)$ shows the NS/BH merger rate at redshift z and τ is the proper look back time of the source. $a_0 r(z)$ and $\frac{d\tau}{dz}$ are given as[34] $a_0 r(z) = H_0^{-1} \int_0^z dz'/\sqrt{\Omega_m(1+z')^3 + \Omega_\Lambda}$, $d\tau/dz = \{H_0(1+z)\sqrt{\Omega_m(1+z')^3 + \Omega_\Lambda}\}^{-1}$, respectively. Following Ref. 34), we adopt the model for $\dot{n}(z)$ given by $\dot{n}(z) = \dot{n}_0 R(z)$, where $\dot{n}_0 = 10^{-8}$ Mpc^{-3} yr^{-1} is the estimated merger rate today and $R(z) = 1 + 2z$ (for z $\leq$ 1), $(3/4)(5 - z)$ (for 1 $\leq$ z $\leq$ 5), 0 (for z $\geq$ 5) encodes the time-evolution of this rate. This model gives the merger rate of 10^4 yr^{-1}. For simplicity, we assume that all NS/BH binaries have the same typical masses of $(1.4, 10)M_\odot$. We first calculate the variance $\sigma(z)$ for various z using pattern-averaged estimate and obtain the total variance σ from Eq. (3). The Fourier component of the pattern-averaged waveform is given by Eq. (29) of Ref. 18). To take into account the effects of redshift, all we have to do is to replace the masses with the redshifted ones: $m_{NS} \rightarrow (1 + z)m_{NS}$ and $m_{BH} \rightarrow (1 + z)m_{BH}$. The distance in this expression is to be understood as the luminosity distance given by $D_L = a_0(1 + z)r(z)$.

From the pattern-averaged analysis, we find that observation of 10^4 binaries with $(1.4, 10)M_\odot$ can put a constraint $\omega_{BD} > 2.18 \times 10^8$. This is 94 times stronger than the one from a single binary placed at 17 Gpc (corresponding to a binary of SNR $= 10$). We calibrate the result of this analysis by using the results of Monte Carlo simulation to yield $\omega_{BD} > 3.77 \times 10^8$. This is 4 orders of magnitude stronger than the current strongest bound.

In Table V, we show the results of error estimation in massive graviton theories

Table V. Results of error estimation in massive graviton theories for $(10^6, 10^5)M_\odot$ BH/BH binaries at 3 Gpc. The meaning of each line is the same as in Table IV.

cases	SNR	λ_g (10^{20} cm)	$\Delta\ln\mathcal{M}$ (%)	$\Delta\ln\eta$	$\Delta\beta$	$\Delta\sigma$	$\Delta\Omega_S$ (str)
pattern-averaged	2044	1.270	1.19	1.69	9.10	2.44	-
no precession	2601	1.266	1.16	1.64	8.92	2.40	1.16
including precession	2666	3.349	0.314	0.0388	0.0612	0.529	0.0248
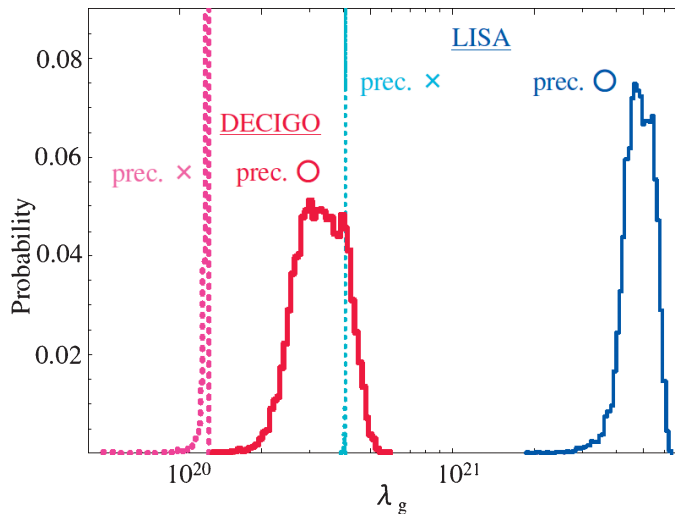
Fig. 3. Histograms showing the probability distribution of the lower bound of λ_g obtained from our Monte Carlo simulations of 10^4 BH/BH binaries in massive graviton theories. We take the masses of the binaries as $(10^6, 10^5)M_\odot$ at 3 Gpc. For comparison, we also show the results obtained in 18) for $(10^7, 10^6)M_\odot$ BH/BH binaries using LISA. The meaning of each histogram is the same as in Fig. 2.

for $(10^6, 10^5)M_\odot$ BH/BH binaries at 3 Gpc with both pattern-averaged analysis and Monte Carlo simulations. Again, we have chosen an optimised mass parameter which can be understood from Table III. The meaning of each row is the same as in Table IV. We can see that the constraint on λ_g increases by a factor of two when we include precession. Figure 3 represents the histograms showing the number fraction of binaries that give the constraint of each λ_g. For comparison, we also show the results obtained in 18) for $(10^7, 10^6)M_\odot$ BH/BH binaries at 3 Gpc using LISA. SNRs for the gravitational waves from these binaries correspond to 1600. The meaning of each histogram is the same as in Fig. 2. We can see that the effect of precession is larger for LISA. We expect that this is because the effective frequency range is wider for $(10^7, 10^6)M_\odot$ BH/BH binaries with LISA. The lower bound on λ_g obtained by DECIGO, 3.35×10^{20} cm, is one order of magnitude smaller than that obtained by LISA. However, this is still three orders of magnitude larger than the one obtained by the solar system experiment. These results show how powerful DECIGO can be in constraining alternative theories of gravity.

Recently, Arun and Will[36)] have estimated the constraint on λ_g including higher harmonics in the waveform. Since they do not include spins, it is important to include both higher harmonics and spin precession, and estimate the constraint on various alternative theories of gravity. This is left for future work.

1) Supernova Search Team Collab. (A. G. Riess et al.), Astrophys. J. **607** (2004), 665.
2) C. Brans and R. H. Dicke, Phys. Rev. **124** (1961), 925.
3) M. Fierz and W. Pauli, Proc. R. Soc. London A **173** (1939), 211.
4) V. A. Rubakov, hep-th/0407104.
5) S. L. Dubovsky, J. High Energy Phys. **10** (2004), 076.
6) V. A. Rubakov and P. G. Tinyakov, Phys. Usp. **51** (2008), 759.
7) e.g., Y. Fujii and K. Maeda, *The Scalar-Tensor Theory of Gravitation* (Cambridge University Press, 2007).
8) B. Bertotti, L. Iess and P. Tortora, Nature **425** (2003), 374.
9) N. D. R. Bhat, M. Bailes and J. P. W. Verbiest, Phys. Rev. D **77** (2008), 124017.
10) C. Talmadge, J. P. Berthias, R. W. Hellings and E. M. Standish, Phys. Rev. Lett. **61** (1988), 1159.
11) C. M. Will, Phys. Rev. D **50** (1994), 6058.
12) C. M. Will, Phys. Rev. D **57** (1988), 2061.
13) P. D. Scharre and C. M. Will, Phys. Rev. D **65** (2002), 042002.
14) C. M. Will and N. Yunes, Class. Quantum Grav. **21** (2004), 4367.
15) E. Berti, A. Buonanno and C. M. Will, Phys. Rev. D **71** (2005), 084025.
16) K. Danzmann, Class. Quantum Grav. **14** (1977), 1399.
17) LISA web page: http://lisa.nasa.gov/
18) K. Yagi and T. Tanaka, Phys. Rev. D **81** (2010), 064008.
19) T. A. Apostolatos, C. Cutler, G. J. Sussman and K. S. Thorne, Phys. Rev. D **49** (1994), 6274.
20) A. Vecchio, Phys. Rev. D **70** (2004), 042001.
21) A. Stavridis and C. M. Will, arXiv:0906.3602.
22) N. Yunes and F. Pretorius, Phys. Rev. D **80** (2009), 122003.
23) N. Seto, S. Kawamura and T. Nakamura, Phys. Rev. Lett. **87** (2001), 221103.
24) S. Kawamura et al., Class. Quantum Grav. **23** (2006), S125.
25) S. Sato et al., J. Phys. Conf. Ser. **154** (2009), 012040.
26) E. S. Phinney et al., *Big Bang Observer Mission Concept Study* (NASA, 2003).
27) C. Ungarelli, P. Corasaniti, R. A. Mercer and A. Vecchio, Class. Quantum Grav. **22** (2005), S955.
28) C. Cutler and D. E. Holz, arXiv:0906.3752.
29) C. Cutler and M. Vallisneri, Phys. Rev. D **76** (2007), 104018.
30) M. Vallisneri, Phys. Rev. D **77** (2008), 042001.
31) A. J. Farmer and E. S. Phinney, Mon. Not. R. Astron. Soc. **346** (2003), 1197.
32) M. Ando, private communications.
33) G. Nelemans, L. R. Yungelson and S. F. Portegies Zwart, Astron. Astrophys. **375** (2001), 890.
34) C. Cutler and J. Harms, Phys. Rev. D **73** (2006), 042001.
35) M. Shibata, K. Kyutoku, T. Yamamoto and K. Taniguchi, Phys. Rev. D **79** (2009), 044030.
36) K. G. Arun and C. M. Will, arXiv:0904.1190.